Benchmarking of Tomographic Reconstruction Systems for Longitudinal Beam Quality in the Proton Synchrotron

Liam O'Shaughnessy
CERN, CH-1211 Geneva, Switzerland

Summary

This document investigates and compares the tomographic reconstruction systems for longitudinal beam quality used in CERN's Proton Synchrotron - the existing Tomoscope application and the newly developed Longitudinal Beam Observation (LBO) system. The presented analysis aims to understand the source of potential differences between the two systems, by investigating discrepancies in each part of the reconstruction pipeline, for different longitudinal beam shapes and energies. This report finds that LBO system is in excellent agreement with the reconstructions from the Tomoscope, with the real discrepancies between the two being minor and likely originating from the acquisition system of the raw data.

Contents

1   Introduction

Within the Proton Synchrotron (PS), injected beams from the Proton Synchrotron Booster (PSB) are accelerated to produce high-energy streams of particles tailored to the requirements of each of the CERN experiments. As the behavior of particles in the beam is complex, and the beam requirements for each experiment specific, a system of accurately measuring beam observables is critical in ensuring the beam quality during operations.

Until 2024, longitudinal beam observation in the PS was performed by an application called Tomoscope [4] [5], which acquires data from beam instrumentation devices (fast digitizer connected to a wall current monitor [3]) and reconstructs the longitudinal phase space of the beam with a tomography algorithm. A more flexible replacement system, the Longitudinal Beam Observation (LBO) system [2], was developed and promises improvement in ease of use, data acquisition, and real-time tomography. This report summarizes comparative investigations into the fidelity of tomographic reconstructions by the two systems.

2   Presentation of the Tomoscope and the LBO system

Reconstruction of longitudinal beam parameters was performed in the following manner via the Tomoscope application (shown in Figure 1): continuous raw beam data was acquired by resistive wall current monitors in the synchrotron at some time in the cycle, which was then digitally transformed by fast digitizers and filtered/triggered on. Specifically, the number of traces can be specified through the Tomoscope application, as well as the number of samples per trace and the sampling frequency. Fetching values like radio-frequency (RF) cavity voltage and harmonic number from the machine, an iterative reconstruction algorithm can be performed on the data to obtain the time-energy phase space (shown in Figure 2) [7] [6] [1]. This phase space then allows for the computation of longitudinal emittance, momentum spread, and other beam parameters [4].

The Tomoscope has various limitations in its usage. First, it is not a pulse-by-pulse modulation (PPM)-based application, meaning that settings have to be shared between different cycles, constraining the number of simultaneous available time windows. In addition, the Tomoscope is an on-demand application that cannot run over an extended period of time or an online manner.
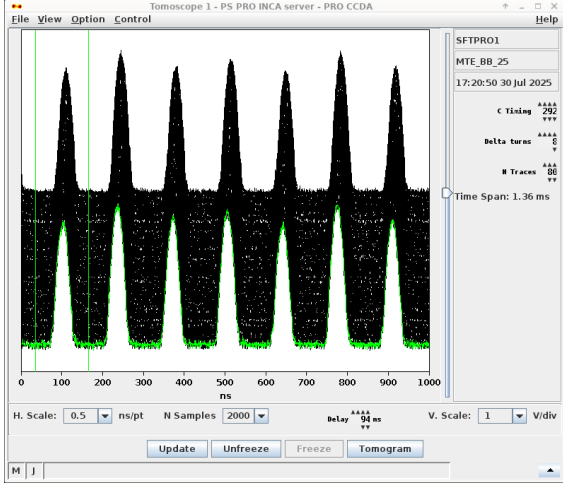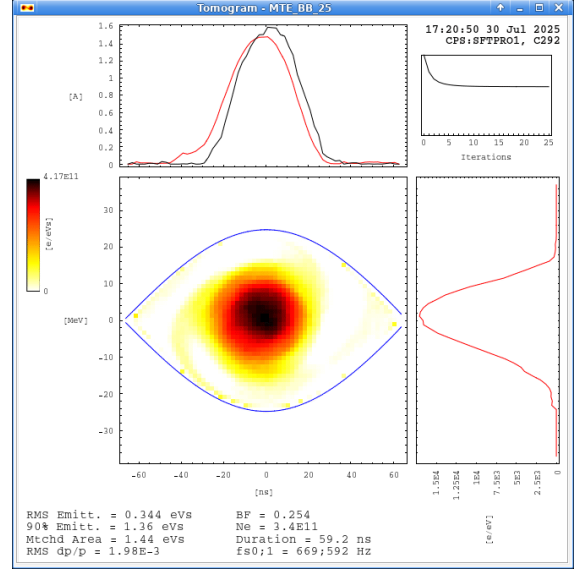
Figure 1: The Tomoscope application.

Figure 2: Phase space reconstructed by the Tomoscope application.

To overcome the limitations of the Tomoscope, the LBO system was developed using the Front-End Software Architecture (FESA) framework in combination with additional post-processing layers for real-time computation of longitudinal metrics using the Unified Controls Acquisition and Processing (UCAP) framework [2]. This system is continuously monitoring each cycle in a PPM manner. The Tomoscope requires the CCM console to select a context to read input, and will only allow up to two consoles to run the application at one time, using the two hardware channels available from the wall current monitor. These maximum of two instances of the Tomoscope being run are designated as "master", and any others are designated as "slave", unable to acquire data.

Conversely, LBO allows the user to be selected and changed within the GUI, independent of the CCM console context. LBO additionally does not have a maximum limit of two windows being open at once. LBO uses a system of 16 independent times of acquisition per cycle in the form of "bursts", able to take readings at different cycle times with configured settings, which allows the user a greater range of measurement. LBO can display data for the entire cycle and can compute bunch-by-bunch tomography in real-time for potentially each of the bursts (shown in Figure 3). Previously, the presets for different moments within a cycle had to be stored as files for each user and had to be tuned each year and manually loaded into the Tomoscope. Now, the LBO system automatically fetches these parameters from LSA settings database directly.
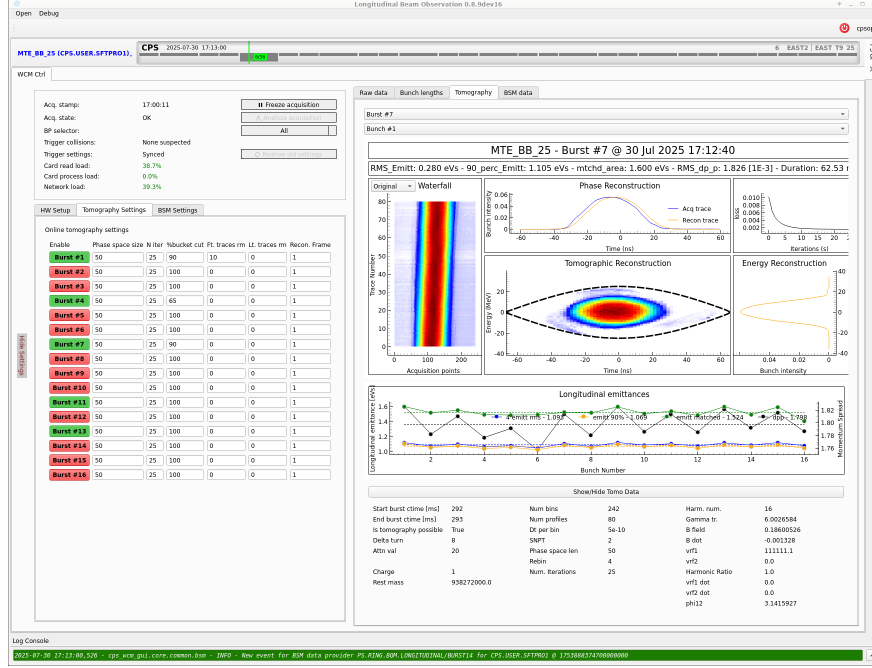
Figure 3: An LBO GUI window

3   Benchmarking method

The BE-OP team wishes to replace the old Tomoscope system with the new LBO one. To effectively perform this replacement, both system results should reasonably agree for each user and configuration. This was investigated by selecting the same user, inputting the same parameters (cycle time, delta turns, number of traces, etc.), and comparing the reconstruction results. Specifically, this can be quantified by examining differences in longitudinal beam parameters such as RMS emittance, 90 percent emittance, matched area, RMS dp/p, and duration. A preliminary comparison indicated that LBO tends to return RMS emittance values that are about 5 to 10 percent higher than those of Tomoscope for different users and different cycle times, as shown in Table 1.

User	Cycle time [ms]	Tomoscope emittance [eVs]	LBO emittance [eVs]	% difference
TOF25	240	0.3618	0.3958	9.4%
TOF25	298	0.5973	0.6355	6.4%
ION2	480	0.1988	0.2193	10.3%
ION3	235	0.1907	0.208	9.1%
EAST2	298	0.4351	0.462	6.2%

Table 1: Average RMS emittances over 6 measurements for different users

In attempting to determine the source of this discrepancy, the reconstruction pipeline was modeled in three parts: acquisition (the WCMs, sampling, digitization, etc.), input

parameter settings (cavity voltages, magnetic field, machine parameters, etc.), and actual reconstruction (tracking, back propagation, etc.). All these parts could add some discrepancy in the end results, and a thorough analysis was required to identify the main drivers.

There existed slight differences in the input parameters between the two systems. For instance, when examining the TOF cycle at a cycle time of 240 ms, the voltage of the main cavity regime might appear as 143992.95 kV in one system, whereas in the other it was 144927.76 kV. The differences were quite small, yet the sensitivity of the systems to the discrepancies was investigated. As a result of this observation, input parameters were forced to be exactly the same, using the LBO parameters given. This produced no change in reconstructed parameters.

Following that, the possibility of differences in "algorithm" was considered - that is to say, the possibility that the tracking and back propagation steps were not identically implemented in the two systems. To eliminate the possibility of this happening, the raw data from Tomoscope and LBO were imported into a Jupyter notebook and run on the same code with the same input parameters. The measured digitizer signals were additionally normalized to ensure the algorithm was not depending on the different analogue to digital signal conversion.
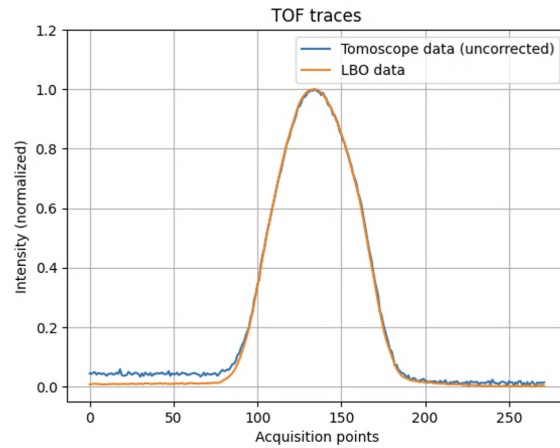

Figure 4: Single raw traces from Tomoscope and LBO of TOF at 240 ms

The waterfall representation of the raw data for the two systems (traces of the beam stacked on top of each other from the time of the burst) showed slightly higher intensities on the earlier part of the traces for Tomoscope, as well as a very brief higher intensity just after the main bunch. The slightly higher intensity above baseline for the Tomoscope can be seen above in Figure 4. These were determined to be due to the transfer function and alignment of the two signals. In the LBO data, the data automatically has a transfer function correction applied to the raw data, while Tomoscope does not. When the transfer function correction was applied with the appropriate inductance and resistance, this earlier part intensity disappeared in the Tomoscope waterfall. Additionally, it appeared that shifting the Tomoscope data acquisition points over when needed in the waterfall plots fixed the brief higher intensity, suggesting an alignment issue between the two data streams. This is shown below in Figure 5.
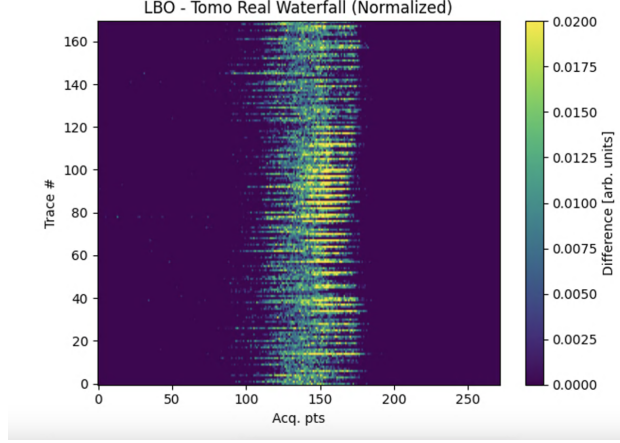
Figure 5: Difference of normalized waterfall plots for TOF 25 240 ms, showing that the traces are differing by less than 0.1 arbitrary units.

To center the data more automatically, handle multi-bunch cycles, and perform the crop in a standard way (as manual adjustments had to be made to vary the shift until there was alignment), the Tomoscope data was split per bunch. This was accomplished by using Scipy's find peaks to identify the average centers of the bunches across the waterfall plot (peak averaged over all traces), and then taking the same number of samples in both directions to match the already-cropped bunch coming from the LBO system (shown below in Figure 6).
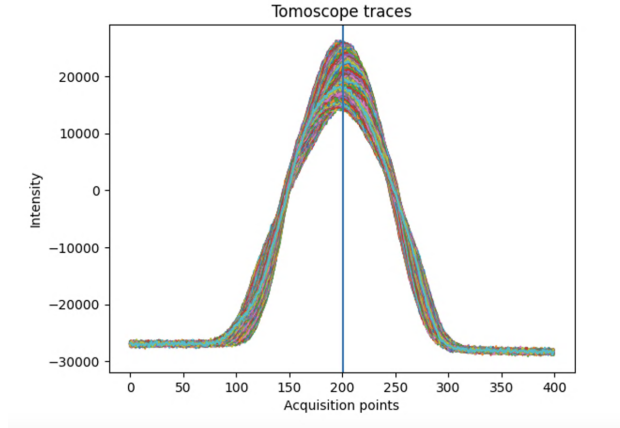

Figure 6: Traces from the Tomoscope over the acquisition window. Splitting per bunch would find n peaks per trace, and then average these to obtain average centers of the n bunches.

While this does group the Tomoscope raw data by bunch, it is not always possible to establish a one-to-one correspondence between individual bunches read by Tomoscope and those read by LBO if the ring is full. Since the scales for points per nanosecond should be the same, Tomoscope runs into an upper limit on its acquisition window when measuring at the same scale as LBO for something like SFTPRO1 (in which case tracking a particular bunch would require a more refined technique than necessary). Hence, the analysis was

not made to compare Tomoscope bunch n to LBO bunch n, but rather the average over the Tomoscope bunches to the average over LBO bunches. The auto-center and auto-crop would appear to have reduced the artifacts found near the separatrix (the region of phase space that separates stable and unstable particles) for Tomoscope as well (this would happen often during the beginning of this investigation). This is shown in Figure 7.
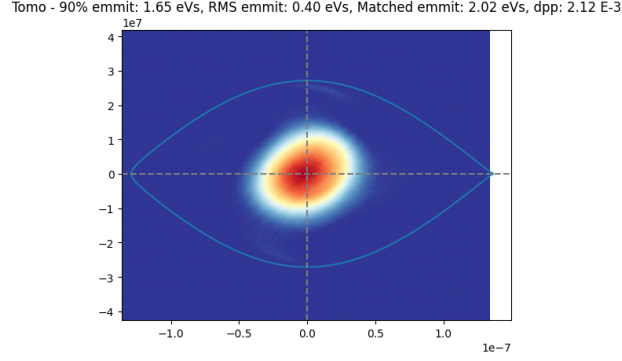

Figure 7: Artifact-free phase space from Tomoscope data for TOF C240

4 Results

4.1 TOF 25 (TOF)

The first user examined was TOF 25 at cycle time 240 ms. This occurs during the intermediate flat bottom. Below are waterfall plots in Figures 8 and 9. When one was subtracted from the other, shown above in Figure 4, the differences appear minimal.
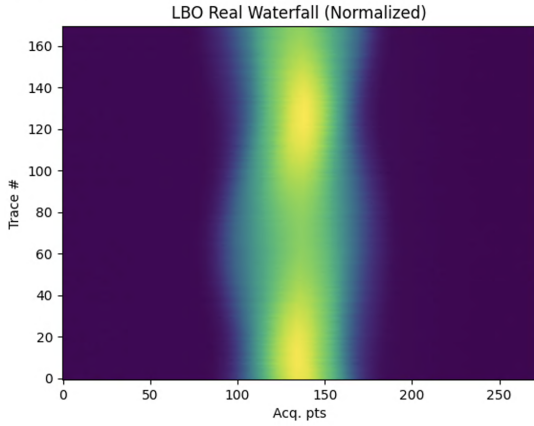

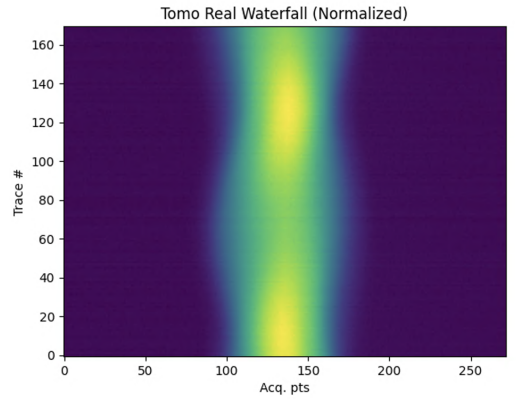Figure 8: Waterfall plot of a bunch from LBO data

Figure 9: Waterfall plot of a bunch from Tomoscope data

The phase space reconstructions for dt on the x-axis and dE on the y-axis also appear normal and similar, as seen in Figures 10 and 11.

7
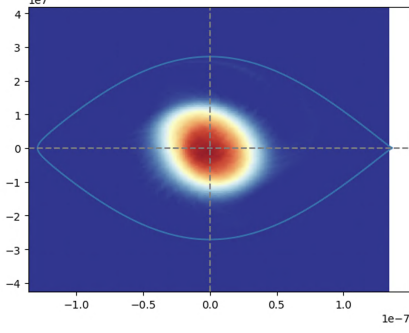
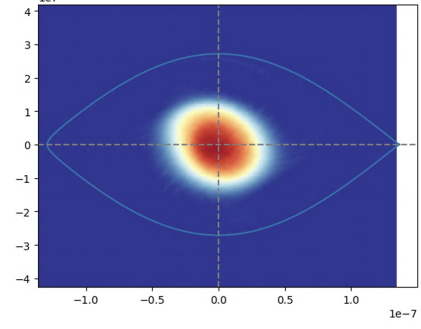Figure 10: Phase space for LBO data

Figure 11: Phase space for Tomoscope data

The exact discrepancies between the reconstructions can be quantified by comparing the difference between reconstructed parameters, averaged over multiple acquisitions. Generally, for a multi-bunch cycle, average values of parameters over the bunches would need to be calculated for each cycle, yet in this case, there is only one bunch to consider. These are highlighted in Table 2.

Parameter	LBO	Tomoscope	% difference
RMS emittance [eVs]	0.4147 ± 0.0066	0.4170 ± 0.0107	-0.55%
90% emittance [eVs]	1.6965 ± 0.0178	1.6751 ± 0.0188	1.28%
matched area [eVs]	2.2900 ± 0.2780	2.2774 ± 0.2714	0.55%
dp/p	0.0021 ± 0.0001	0.0021 ± 0.0001	0.0%
bunch duration [ns]	99.8524 ± 6.5435	99.5624 ± 6.3782	0.29%

Table 2: Average and standard deviation for parameters for C240 burst

4.2 MTE BB 25 (SFTPRO1)

MTE BB 25, which during the time of this analysis was labeled as user SFTPRO1, was examined at cycle time 790 ms (near the end of flat top). This beam uses a full ring with 8 bunches, so bunches cannot be matched for reasons mentioned above (without intensive comparison, which would be more time-intensive than fruitful). The following waterfall plots in Figures 12 and 13, hence, are from different bunches.
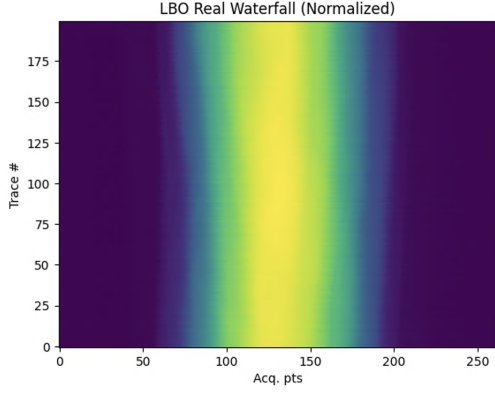
8

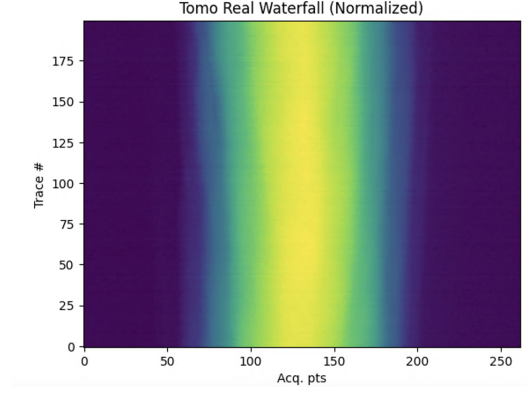Figure 12: Waterfall plot of a bunch from LBO data

Figure 13: Waterfall plot of a bunch from Tomoscope data

Examining the full phase space in Figures 14 and 15, both look similar and reasonable. However, note the minor artifacts near the separatrix in the phase space for the Tomoscope data.
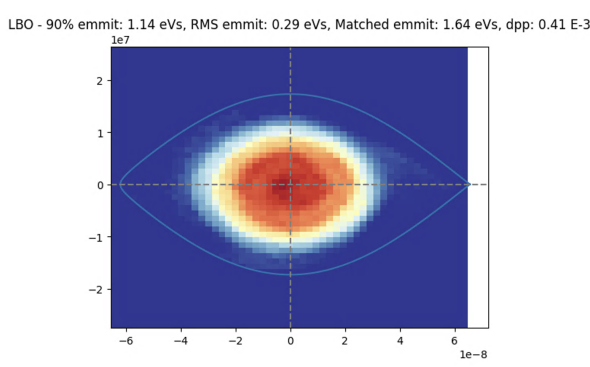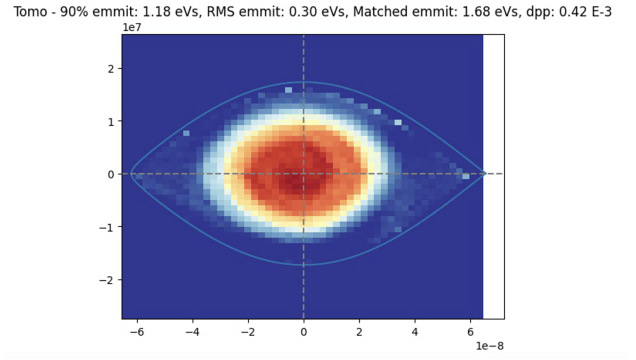

Figure 14: Phase space for bunch from LBO data

Figure 15: Phase space for bunch from Tomoscope data

Computing the average parameter values for the two systems, taking into account averaging over bunches in each burst, yields the following in Table 3. Note that, due to the sampling limit of Tomoscope at this scale, not every bunch was able to be included in the data capture, so the averaging is only done over a subset of bunches for the Tomoscope data, while it is done over all bunches for LBO. This is assumed to not be statistically impactful.

Parameter	LBO	Tomoscope	% difference
RMS emittance [eVs]	0.2799 ± 0.0042	0.2867 ± 0.0037	-2.37%
90% emittance [eVs]	1.1162 ± 0.0173	1.1289 ± 0.0139	-1.12%
matched area [eVs]	1.5851 ± 0.0215	1.5967 ± 0.0130	-0.73%
dp/p	$0.0004 \pm 4*10^{-6}$	$0.0004 \pm 4*10^{-6}$	0.0%
bunch duration [ns]	76.5633 ± 0.6480	76.9116 ± 0.3926	-0.45%

Table 3: Average and standard deviation for bunch-averaged parameters for C790 burst

4.3   LHC25#48b BCMS LowTail 25 (LHC3)

Finally, LHC25#48b BCMS LowTail 25, assigned at this time to the name LHC3, was considered. Examining at cycle time C2842 at flat top, when the beam had been split into 36 bunches, the waterfall plots in Figures 16 and 17 appear as expected (bunches can now be compared directly, as the ring is not full, and there is a clear observable "start" to the beam).
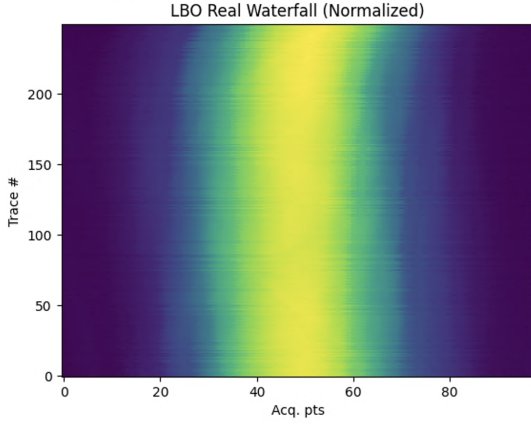

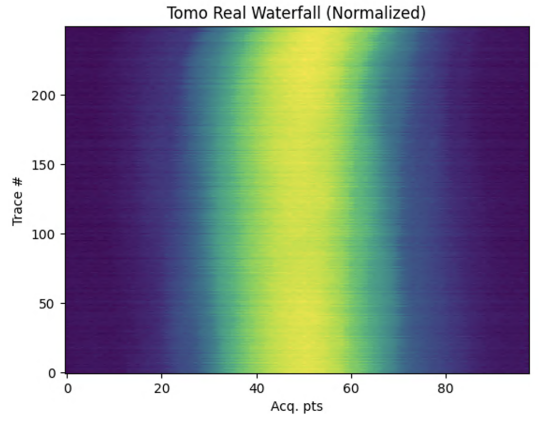Figure 16: Waterfall plot of bunch 1 from LBO data

Figure 17: Waterfall plot of bunch 1 from Tomoscope data

The reconstructions appear very similar for both LBO and Tomoscope in Figures 18 and 19.
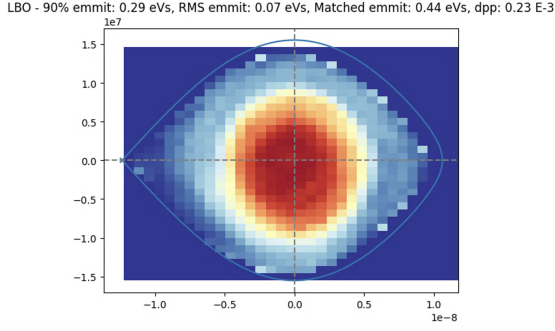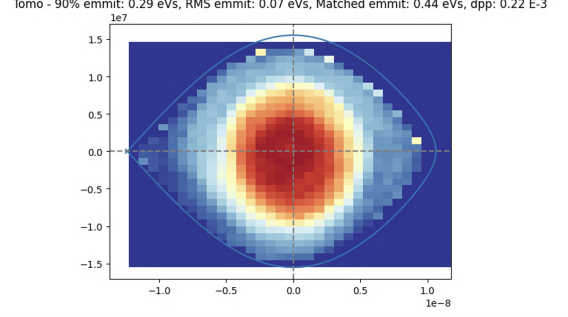
Figure 18: Phase space for LBO bunch 1

Figure 19: Phase space for Tomoscope bunch 1

Finally, the averaged statistics were calculated in Table 4. Note that a subset of bunches were used for the Tomoscope.

Parameter	LBO	Tomoscope	% difference
RMS emittance [eVs]	0.0660 ± 0.0011	0.0650 ± 0.0014	1.54%
90% emittance [eVs]	0.2757 ± 0.0053	0.2715 ± 0.0056	1.55%
matched area [eVs]	0.4112 ± 0.0055	0.4066 ± 0.0069	1.13%
dp/p	$0.0002 \pm 1 * 10^{-6}$	$0.0002 \pm 2 * 10^{-6}$	0.0%
bunch duration [ns]	19.3999 ± 0.2242	19.2111 ± 0.2717	0.98%

Table 4: Average and standard deviation for bunch-averaged parameters for C2842 burst

5 Discussion

At various cycle times for various users, it would appear that the Longitudinal Beam Observation system recovers similar values to Tomoscope. The LBO averages differ from the Tomoscope averages by, at maximum, 2.37%. In many cases, the difference is 1% or less - performing two-sample t-tests for each parameter yields very large p-values, signifying lack of evidence that the reconstruction parameters from the two systems follow different distributions. When factors such as the transfer function and common inputs are imposed, the apparent differences observed preliminarily shrink greatly. It would appear, all else being reasonably equal and addressed, that the discrepancies remaining result from differences in the acquisition hardware.

Consequently, it appears that LBO effectively performs tomographic reconstruction of longitudinal beam parameters, with better data quality, data processing, and ease of use. It seems reasonable that this system be used for tomography, not only in the Proton Synchrotron but also other accelerators at CERN, moving forward.

6 Acknowledgements

References

[1] S. Albright C. Grindheim. Longitudinal phase space tomography version 3. *CERN Document Server*, 2021.

[2] Amaury Beeckman et al. Real-time monitoring of longitudinal beam quality across the cern accelerator complex. *Elsevier (preprint)*, 2025.

[3] P. Forck. Lecture notes on beam instrumentation and diagnostics. 2023.

[4] J.-L. Sanchez Alvarez J.-F. Comblin, S. Hancock. A pedestrian guide to online phase space tomography in the cern ps complex. *CERN Document Server*, 2003.

[5] M. Ruette J.L. Alvarez. Ps bunch shape measurement. *CERN Document Server*, 1998.

[6] C. Grindheim-A. Lu S. Albright, A. Lasheen. Recent developments in longitudinal phase space tomography. *Journals of Accelerator Conferences*, 2022.

[7] M. Lindroos S. Hancock, P. Knaus. Tomographic measurements of longitudinal phase space density. *CERN Accelerator Conference*, 1998.